Detecting Strong Ties Using Network Motifs

Rahmtin Rotabi
Cornell University
rahmtin@cs.cornell.edu

Krishna Kamath
Twitter Inc.
kkamath@twitter.com

Jon Kleinberg
Cornell University
kleinber@cs.cornell.edu

Aneesh Sharma
Twitter Inc.
aneesh@twitter.com

ABSTRACT

Detecting strong ties among users in social and information networks is a fundamental operation that can improve performance on a multitude of personalization and ranking tasks. There are a variety of ways a tie can be deemed "strong", and in this work we use a data-driven (or supervised) approach by assuming that we are provided a sample set of edges labeled as strong ties in the network. Such labeled edges are often readily obtained from the social network as users often participate in multiple overlapping networks via features such as following and messaging. These networks may vary greatly in size, density and the information they carry — for instance, a heavily-used dense network (such as the network of followers) commonly overlaps with a secondary sparser network composed of strong ties (such as a network of email or phone contacts). This setting leads to a natural strong tie detection task: given a small set of labeled strong tie edges, how well can one detect unlabeled strong ties in the remainder of the network?

This task becomes particularly daunting for the Twitter network due to scant availability of pairwise relationship attribute data, and sparsity of strong tie networks such as phone contacts. Given these challenges, a natural approach is to instead use structural network features for the task, produced by *combining* the strong and "weak" edges. In this work, we demonstrate via experiments on Twitter data that using only such structural network features is sufficient for detecting strong ties with high precision. These structural network features are obtained from the presence and frequency of small network motifs on combined strong and weak ties. We observe that using motifs larger than triads alleviate sparsity problems that arise for smaller motifs, both due to increased combinatorial possibilities as well as benefiting strongly from searching beyond the ego network. Empirically, we observe that not all motifs are equally useful, and need to be carefully constructed from the combined edges in order to be effective for strong tie detection. Finally, we reinforce our experimental findings with providing theoretical justification that suggests why incorporating these larger sized motifs as features could lead to increased performance in planted graph models.

.

Keywords

strong-tie detection, graph information transfer, network motifs

1 Introduction

Many large social media platforms are constructed so that users participate in multiple networks simultaneously. On Twitter, for example, a user can establish links to other users by following them, or sending them a direct message, or by including them in a phone book or e-mail address book. Each of these modes of interaction defines a different network on the set of users — while these networks are clearly related, they represent different types of connections; you might easily follow someone whom you have no expectation of ever messaging or contacting by phone. Moreover, the networks can differ greatly in their usage and sparsity; Twitter users will generally follow multiple other users, but many may have never populated their phone books.

In these social media contexts, we thus encounter a wide range of cases in which a network G_L with a large number of links coexists with an overlapping, but much sparser network G_S. As in the case of the (dense) follower graph and (sparser) phone book graph on Twitter, the sparsity of G_S often comes about for two reasons. First, in contrast to the follower graph, the phone book is not the main feature of the site. Second, even for users who have created links in the sparser graphs G_S (such as the phone-book graph), these links tend to correspond to the user's *strong ties*, and so are less numerous. Despite their sparsity, networks like the phone-book graph contain information that is immensely valuable, in part because of their focus on strong ties; they can be used for improving relevance and personalization in user/content recommendations, creating more personalized notifications, and other applications. Many of these tasks can benefit from estimates of edges likely to belong to G_S, even if they haven't been explicitly reported by users.

Thus, estimating which edges belong to these types of sparse graphs G_S can be viewed as a type of strong-tie detection problem [9]. But as we discuss next, our setting adds new aspects to the problem; existing techniques for strong-tie detection produce weak performance in our context, and in contrast we develop a set of new methods that yield significantly more powerful results.

Data-driven strong tie detection Our particular setting of the Twitter network adds some new dimensions to strong tie detection that we believe haven't been studied before in concert: (i) a data-driven formulation of the problem; (ii) extreme sparsity of demographic features; and (iii) possible ineffectiveness of interaction features. The first point here is that while the sparse graphs G_S that we consider have significant overlap with the strong-tie structure, they are not precisely the set of strong ties, and so we need to take a data-driven approach: rather than starting from sociological principles about strong-tie structure, we use the existing structure of edges around nodes that participate in G_S to learn the features that are most predictive, The second and third points, about the limitations of demographic and interaction features for our problem, make clear why new techniques are needed. Recall that these kinds of features (reciprocity of interaction, engagement volume, and related measures) have been proven to be the most effective at strong tie detection in prior work [9]. But in our setting, the demographic features are quite sparse as users do not need to report demographic information to use the website. Furthermore, due to the data-driven approach, interaction features may not be most indicative of the particular strong tie label we're trying to predict.

As a concrete way to see the challenge, we began by running standard strong-tie detection algorithms using as many features from existing methods [9] as we could (all the high-weight features were available), trying to predict whether an edge in the Twitter follower graph was also in the phone-book graph. We found that on a fully balanced dataset these features only provide a prediction accuracy of 56% which barely beats the random baseline by 6%. As we will show in this work, we are able to do much better with the techniques we develop here; our eventual performance will be 87% accuracy for the same task. Given the poor performance of prior baselines, it becomes important to understand the challenges in this particular version of the problem more clearly.

In the motivating applications for the problem, the graph G_S providing the strong tie labels is sparse because many (or most) users have not yet started using the feature defining G_S, leading to a graph with a large fraction of disconnected or isolated nodes. And even the nodes that are not isolated have very low degrees. As a result, standard link-prediction methods cannot be applied on G_S alone to "bootstrap" the internal structure of G_S by itself.

Our setting is closer to the "cold-start" problem in recommendation systems [2, 23, 24], where the challenge is to make recommendations to users for whom the system has no history at all, and the general idea is to use some source of side information to provide recommendations to such users. This is where the weak ties provided by the denser network G_L come into play; even if a user u has no edges in G_S, the weak ties that u has in G_L provide information about the presence of u's edges in G_S. We note that in contrast to prior work on the cold-start problem, our side information in this case is a network in its own right. In this respect, our strong tie detection problem is a question of information transfer. In contrast to existing work on information transfer, however, we are considering settings where we may well not have any a priori principles informing the typical patterns of links in our domain. Thus, we aim to induce patterns purely from training data, adapting to different settings independently of whether any particular hypothesized structural patterns turn out to be the most effective.

The core of our problem, then, is to combine information from the weak ties in G_L with the strong ties from the subset of nodes that participate in G_S, to predict strong ties for nodes that currently do not participate in G_S. We now discuss some of our techniques and results for this problem.

Filling in a sparsely-populated network Addressing this question requires that we use information latent in both G_S and G_L. Intuitively, from the portions of G_S that we are able to observe, we try to infer the typical patterns formed by the edges in G_S and their interplay with edges in G_L. We then go to nodes where the edges of G_S are absent, and we look for evidence of similar patterns among the edges of G_L. This provides evidence for where the hidden edges of G_S might be. For this strategy to work, it is important that G_L provide us with sufficient information about G_S; a key aspect of the approach is based on transferring information between the two graphs G_L and G_S. In particular, for the "patterns" formed among the edges of G_S, we use the presence of small subgraphs or *motifs* that are highly represented in the observable portion of G_S. Given a user a who is incident to no edges of G_S — a user with no strong ties — we try to infer which of a's incident edges (or weak ties) in G_L are most likely to belong to G_S as well. To do this, we assign each of a's incident edges in G_L multiple scores based on their participation in certain small subgraphs. Note that the edges of these subgraphs may have mixed membership in G_L and G_S; in particular, if (a, b) is an edge of G_L, then b may have incident edges in G_S even though a does not.

Using the subgraph-induced scores for an edge (a, b) as a vector of features, we can then learn a classifier for labeling edges of G_L as strong ties based on the nodes in the graph that have incident edges from G_S. In this way, we are not presupposing which particular motifs are indicative of membership in G_S, but instead identifying the most important motifs from the data.

In evaluations on the Twitter user network, we obtain strong performance in inferring the presence of unobserved labels in several of the site's main underlying networks, using *only* network features. In particular, adopting an evaluation framework in which we hide the presence of a subset of the direct messages, phone book, and email address book edges — thus providing ground truth for our evaluation — we find that our approach using the mutual following graph as G_L yields high accuracy in detecting strong ties.

Moreover, among the graph motifs that are most important for the task of classifying edges of G_S, we find that motifs on more than three nodes play a crucial role. This forms an intriguing contrast to the work on strong-tie detection within networks of weak ties — one of the most widely-studied cases of information transfer between different types of networks — since in that context the key issue has traditionally been the participation of an edge (a, b) in triangles, which correspond in our framework to features comprised entirely of a set of three-node subgraphs. For the networks we infer here, the participation of edges (a, b) in larger motifs turns out to be vital as well.

The role of larger graph motifs A possible reason for the role of larger graph motifs in our task is that these larger structures provide a partial antidote to the problem of sparsity — due to the number of combinatorial possibilities, they have the potential to be more abundant than triangles in the training data we have on G_S, particularly when the observed part of G_S is highly sparse. To understand the trade-off between sparsity and the use of larger structures as features, we propose and analyze a set of generative network models where this effect appears clearly, and with provable guarantees. Specifically, we consider a mathematical model in which nodes belong to planted communities, and edges of G_S lie within these communities. As in prior work on random graphs with planted community structure, we cannot directly observe community membership (a proxy for strong ties), but the structure of the graph conveys latent information about it. Our question, however, is related to but different from the standard problem of inferring community membership; rather, we want to classify edges by their membership in G_S, where the random generation of G_S is based on the community structure.

We discover that the qualitative findings from our evaluation on the Twitter dataset hold for this generative model as well, and with provable guarantees arising from analysis of the model; motifs larger than triangles provably help in identifying edges of G_S, and the gain from these subgraphs increases as the observable portion of G_S becomes sparser. Moreover, our approach based on the frequency of motifs is robust enough that it even yields guarantees when nodes belong to multiple overlapping communities with independent membership.

Overall, the interaction of the computational evaluation on Twitter and the analysis of the generative models suggests that our concrete task, transferring information from one graph to discover strong ties around isolated nodes in another, is a useful and general problem that provides insight into the role of local network motifs.

In the remainder of the paper, we first present an experimental evaluation of our methods on the Twitter dataset, followed by modeling and simulations that seek to provide a theoretical basis for understanding our experimental observations.

2 Related Work

Our approach is related to several lines of research concerned with network structure, particularly in the domain of social and information networks. More specifically, our work can be seen as positioned at the intersection of three topics in network analysis: (a) strong tie detection (albeit under extreme sparsity of features), (b) link prediction in a case where many nodes are isolated (because they do not yet participate in G_S), and (c) graph information transfer in a purely data-driven manner, i.e. without pre-supposing any sociological basis.

As we discussed in the introduction, previous work on strong tie detection [10, 9, 18] yields only limited effectiveness in our setting both due to feature sparsity (even of small network motifs such as triads) and due to our data-driven labeling goal; we seek to transfer information from a denser graph on the same set of nodes. Existing methods for strong-tie detection have used structural information based on triangles, following ideas from sociology [11, 18, 6, 13, 26], whereas we make use of motifs larger than triangles. Other studies that have looked at information transfer include analysis of advisor-advisee relationships [30], romantic relationships [1], and other types of relationship transfer [17, 27, 28]. Our goal, however, is to transfer information without a priori sociological principles to guide the process.

A number of fields have developed frameworks for analyzing small subgraphs that occur frequently in larger networks; such formalisms have been termed *network motifs* [20], the *triad census* [7], and *frequent subgraph mining* [16, 31], and have been used in extremal graph theory [3] and social media analysis [29]. Our work takes a different perspective as its starting point; rather than using the frequency of a given subgraph as the key criterion, we are proceeding in a more supervised fashion, using data to infer which subgraphs are most informative for our task.

Another relevant line of work is the network completion problem [14, 15]. Results in this area propose generative models recreating an entire graph to infer missing parts of a given partial graph. These methods have also been developed primarily without the goal of handling a large fraction of isolated nodes; and they only scale up to hundreds of thousand of nodes, which is much smaller than our graphs of interest.

The transfer of graph information bears a distant relationship to transductive learning [12] and label propagation [32], although these methods typically propagate node attributes from labeled to unlabeled nodes, while we use the network structure to infer information about edges. The structure of our generative models draws motivation from *stochastic block models* [4, 19, 21, 22]; for us, such models provide a setting in which phenomena we observe in our computational evaluation appear with provable guarantees, providing a certain level of qualitative insight into how they operate.

3 Methods and Experiments

We now describe our methods for predicting strong ties by combining information from two different graphs G_L and G_S, and we discuss the results of experiments on the Twitter graph.

3.1 Prediction Task

We begin with the formal set-up for our prediction task. Recall that we are given two graphs: a denser graph $G_L = (V, E_L)$ that contains all the edges available to us for analysis; and an overlapping, sparsely populated graph $G_S = (V, E_S)$, which contains the reported strong ties. We will think of the edges in E_S as being *labeled* with their strong-tie status. Recall that one of our primary motivations is to detect strong-tie labels for users who have not reported any strong ties. However, to set up a formal prediction task, we need a ground-truth labeled set that we can compare our predictions to. Thus, we propose the following evaluation framework to evaluate methods for predicting strong ties. We pick a small set of test nodes $V_{\text{test}} \subset V$ and remove all of their edges in E_S while retaining their edges in E_L. Doing this process will simulate the setting where we do not have any strong ties reported around the test nodes. The prediction task for a supervised machine learning algorithm is to build a model on the remaining graph that is able to predict for each $v \in V_{\text{test}}$, which of v's edges in E_L was a removed edge from E_S.

Let $d_L(v)$ denote the degree of node v in G_L, and let $d_S(v)$ denote the degree of v in G_S. Our test set of nodes V_{test} is a random subset of the nodes in V subject to the condition that $d_S(v) > 0$ for all $v \in V_{\text{test}}$. We define $V_{\text{train}} = V - V_{\text{test}}$. We call the induced graph of G_i (again, $i \in \{L, S\}$) on V_{train} and V_{test} to be $G_{i,\text{train}}$ and $G_{i,\text{test}}$, respectively.

To reflect a scenario in which nodes in V_{test} are users who have not adopted the feature that grants us E_s, we allow the algorithm to only utilize $G_{L,\text{train}}$ and $G_{S,\text{train}}$ for training a model. Once the algorithm trains its model, it is given access to $G_{L,\text{test}}$ and the algorithm's prediction task is to output exactly one edge for each node $v \in V_{\text{test}}$, namely the edge that is the algorithm's best guess for belonging in $G_{S,\text{test}}$. The precision of the algorithm for a given set of test nodes is the fraction of correct guesses; in traditional information retrieval parlance it is known as precision in the first position, or $p@1$. Thus, we are considering a setting in which a user joins the platform and links to a few people in the heavily-used network G_L, but does not adopt the sparsely-used network G_S; based on this, we wish to report a link that is likely to be a strong tie for this user.

3.2 Twitter Dataset

We now describe the graphs that we analyze, all of which are produced by interactions between users on Twitter.[1] We study four undirected graphs built from different types of interactions between users on Twitter. The nodes in these graphs are the Twitter users (note that a user may not correspond to an individual, since other account types are possible on Twitter), and the interpretation of the edge depends on the graph being considered. The graphs are as follows:

- **Mutual Follow:** this is the graph of users who follow each other on Twitter. Since we focus on symmetric relationships on Twitter, this results in an undirected graph.
- **Phone Book:** Twitter users often import their phone books for finding their friends on Twitter. That feature gives rise to a graph in which we have an edge between two users if and only

[1]All the Twitter data has been analyzed in an anonymous, aggregated form to preserve private information.

if both users have imported their phone book and have each other's phone number.

- **Email Address Book:** users can also import their email address book on Twitter, and analogous to the phone book, we can construct an email graph where an edge exists if both users have each other in their email address book.
- **Direct Message:** Users on Twitter can also send private messages to each other, and these are called *direct messages*. Thus, we can consider an undirected graph in which there is an edge between each pair of users who have sent at least one direct message to each other.

For our computational experiments, we collected a single complete snapshot of all these graphs on July 30, 2015. The mutual follow graph contains hundreds of millions of users, and tens of billions of edges. The portion of other graphs that we consider are approximately a tenth the size of the mutual follow graph.[2] As the Mutual Follow graph is much more densely populated than the others, we create three instances of our prediction task: in each, the Mutual Follow graph forms G_L, and one of the other graphs (Phone Book, Email Address Book, or Direct Message) forms G_S. We only preserve edges in G_S that also belong to G_L; this removes less than 0.5% of edges, so it is a simplification with negligible impact for our purposes.

We construct V_{test} by randomly choosing 5% of the nodes that satisfy the following pair of conditions: (i) they have an edge in G_S, and (ii) their degree in G_L is between 10 and 75. This degree restriction on G_L reflects the motivating scenario in which the users in V_{test} are relatively lighter users (or new users) of the platform, for whom we are trying to infer edges in networks they have not yet populated (while still having enough edges to predict). The smallest V_{test} over the three different graphs we look at includes roughly 29000 nodes.

3.3 Prediction Algorithms

Our algorithms for predicting strong ties will operate as follows. We start with a node $a \in V_{\text{test}}$ that has no incident edges in G_S, and we would like to identify an edge in G_L, incident to a, that in fact belongs to G_S. Let B be the set of neighbors of a in G_L. Because of the simplifying assumption, motivated above, that $E_S \subseteq E_L$, the candidate edges incident to a that we are choosing among all consist of edges from a to a node in B.

We develop a number of *score* functions, each of which assigns a number to every node in B. We can use each individual score as a predictor in itself, by sorting the nodes in B according to the score, selecting the highest-scoring $b \in B$, and declaring (a, b) to be the predicted edge in E_S.[3] A few of these scoring functions are used in the literatures on strong tie detection and on link prediction, and we use them as baselines. Recall from the introduction that interaction features under-perform, so these are in fact stronger baselines for the prediction task. We also use the scores as features and combine them using a machine-learning algorithm trained on the nodes in V_{train} for which we have ground-truth edges belonging to E_S. By comparing the performance of different scores, as well as combinations of them, we can thus determine which structures are most effective at transferring information from G_L to the unpopulated parts of G_S. The fact that our scores include standard baselines from link prediction and strong-tie prediction enables us to quantify the gains from scores corresponding to more complex structural formulations.

In order to define our scoring functions, we introduce the following notation. Given a graph G and a node v in the graph, we use $N(G, v)$ to denote the neighbors of v in G and the operator $\mathbf{Ego}(G, v)$ to refer to the *ego network* (the induced subgraph on $N(G, v) \cup \{v\}$) of the node v in G. Recall that we use a for the node in V_{test} for whom we are predicting an edge in E_S, and $B = N(G, a)$. We also use C to denote the set of nodes at distance exactly two from a in G_L. The scoring functions we use are given in Table 1. We divide the scoring functions into two groups, Group 1 and Group 2. In both groups, we also include a composite score that uses linear regression to combine all the scores (and their logarithms) in the group to form a single machine-learning classifier. Scoring functions in *Group 1* are standard benchmarks from link prediction and strong-tie prediction, and they provide a baseline for comparison. Scoring functions in *Group 2* use larger graph-theoretic structures; where the Group 1 scores are based primarily on triangles and counts of mutual neighbors, the scores in Group 2 use counts of 4-node structures (squares) and 5-node structures (pentagons), with the formal specifications provided in Table 1. We also counted network motifs such as the complete graph of size 4 and 5 but they were too sparse and did not help the prediction.

Before presenting our results, we illustrate the scoring functions with a toy example. In Figure 1, the dashed edges represent weak ties and the solid edges represent strong ties. Note that edges labeled as strong ties also count as weak ties. Consistent with the no-

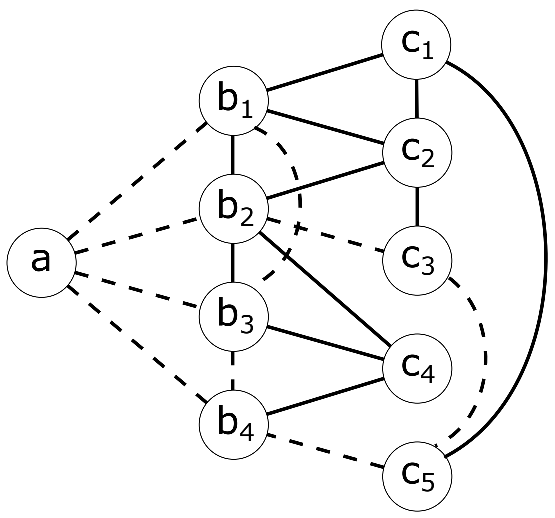

Figure 1: A simple graph centered around node a.

tation above we are looking at node a and all the strong ties of a are hidden. The scores for node b_1 on this small graph are: Degree=5, Embeddedness=2, Adamic-Adar= $\frac{1}{\log(5)} + \frac{1}{\log(6)}$, H1=5, Triangles=1, Square Inside= 1 (Square through b_2 and b_3), Square Outside=1 (Square through c_2 and b_2), Pentagon Inside=0 and finally Pentagon Outside=1 (Pentagon through c_1, c_2 and b_2).

The focus of this work is on finding useful scoring functions for prediction, but we also want to briefly mention computational considerations for these. Computing small sub-structures such as triangles, squares and pentagons on large graphs is well-known to be a challenging problem; the triangles case in particular has a large literature and many provably efficient approximations [25]. We

[2]We are unable to share the exact size of these graphs but we note the relative sparsity of the strong tie graphs.

[3]We break ties based on degree (smaller is prioritized) and the time the user joined the platform (earlier is prioritized).

Table 1: The definition of all the scoring algorithms evaluated experimentally.

Name	Definition	Optimization	Group
Random neighbor	A simplistic baseline that picks a node in B uniformly at random	N/A	1
Lowest degree neighbor[5]	Picks the node $b \in B$ with the minimum degree $d_L(b)$	minimization	1
Embeddedness	Picks the node $b \in B$ that has maximum number of mutual neighbors with a	maximization	1
Adamic-Adar	The score assigned to $b \in B$ is $\sum_{v \in \{B \cap N(G_L, b)\}} \frac{1}{log(d_L(v))}$ which is a weighted version of Embeddedness giving a greater weight to mutual neighbors with a lower degree	maximization	1
H1	This heuristic function assigns $d_L(b)$ as the score for $b \in B$ if $d_S(b) > 0$ and 0 otherwise	minimization	1
Triangle	This method finds $N(G_S, b) \cap B$ for every $b \in B$	maximization	1
Basic ML model	This method builds an LR model using features from rows above	maximization	1
Square inside	For every $b \in B$, this algorithm reports the number of cycles with 4 nodes (or *squares*) containing the edge (a, b) with the other two nodes in the cycle also being in B.[6]	maximization	2
Square outside	For every $b \in B$, this function reports the number of cycles with 4 nodes (or *squares*) containing the edge (a, b), exactly one other node in B and one node in C.[6]	maximization	2
Pentagon inside	This method counts the number of cycles of length 5 for each $b \in B$ containing edge (a, b) where all 5 nodes are inside $\mathbf{Ego}(G_L, a)$.[6]	maximization	2
Pentagon outside	This method counts the number of cycles of length 5 for each $b \in B$ containing edge (a, b) where 3 nodes are inside $\mathbf{Ego}(G_L, a)$ and the other nodes are in C.[6]	maximization	2
Enhanced ML model	This method builds an LR model using all scores listed above as features	maximization	2

briefly note that for practical purposes, heuristics based on neighborhood sketches such as HyperLogLog [8] can be used to efficiently compute these features in a MapReduce [5] computation. We provide a brief description of this heuristic in section 7.1. We emphasize however that in our experiments, we do not use any approximations since our training/test data size was small enough to be tractable with exact computation.

3.4 Performance on Prediction Task

We evaluated each of the scoring algorithms presented in Table 1 on the prediction task outlined above, in which we seek to predict a single edge in E_S incident to the given node a. We present the results in terms of their *precision* — the fraction of instances on which the predicted edge indeed belongs to E_S. Rather than providing just an overall precision number, we present our results grouped according to the degree of the node a. This is to reflect the fact that there is a gradation based on difficulty: nodes of higher degree naturally form harder instances for some algorithms, since there are more candidate edges to choose from (for instance, the baseline of random guessing goes down correspondingly). On the other hand, some algorithms are able to efficiently exploit more available information from the larger neighborhood, and hence this presentation highlights the dependence of our methods on degree.

The precision results are shown in Figures 2 and 3. Note that in these figures, we organize the algorithms according to the Group classification in Table 1, discussed above. As seen in figure 3, the Enhanced LR model performs much better than the Simple LR model that combines all the other baseline algorithms that were proposed previously in the literature. We highlight that there is a large 17%, 12% and 10% gain in precision in the direct message, phone book and Email prediction task, respectively. And it is important to note that we achieve these gains only by adding slightly larger network motifs falling entirely inside or one step outside the ego-network. We emphasize the raw precision value here as well — a priori it would seem that a precision of 75% for phone book prediction using just the network motifs would be too much to ask. The results speak for the power of the motifs approach.

We now discuss further the performance of the algorithms in *Group 2*, depicted in Figure 3. These algorithms differ from the Group 1 benchmarks based on prior work in two aspects: (a) they look at richer motifs in the ego network, such as squares and pentagons, and (b) they also look beyond the ego-network for computing the scores. First, we observe that looking at the richer motifs even in the ego-network is fruitful as the *squares inside* and *pentagons inside* algorithms outperform the triangle algorithm, albeit only slightly. However, the results from looking beyond the ego-network, as demonstrated by the *squares outside* and *pentagons outside* algorithms, are mixed. Only in the email graph does the *squares outside* algorithm beat the others comprehensively. Intuitively, looking beyond the ego-network results in a trade-off between sparsity and signal strength: the signal strength of structures trails off with increasing distance from the ego network, but the number of structures found increases due to increasing combinatorial possibilities. From the results, it seems that the square motifs potentially are a “sweet spot” in this trade off, and we investigate this issue in the next section in more depth. It is evident from the performance results shown in Figure 3 that the LR models outperforms all the other methods and the model using the Group 2 features outperforms the model using Group 1 features from prior work. In examining the enhanced LR model, we find that three significant features in the model that we learned are $\log(square\text{-}inside)$, $\log(square\text{-}outside)$ and $\log(triangles)$. Since the LR model outperformed both these individual features as well, this suggests that the model is combining information from inside and outside the ego network. And this combined algorithm achieves a much higher precision compared to individual scores. Of course, the LR model has access to more features than any individual score; but one might still not apriori expect the features from inside and outside the ego network to complement each other enough to achieve this level of increased precision.

We also note that results on the email graph are a bit different from the other two. In particular, the lowest-degree neighbor algorithm is worse than the random neighbor algorithm on the email graph, and the square-outside algorithm performs better than the square-inside algorithm (and all others for that matter). We hypothesize that this might be due to the noisy nature of the email graph compared to direct messages and phone book. Namely, presence in another user’s email address book is a much weaker signal than having a private conversation or being in another user’s phone book. Finally, we observe that precision is often lower for high degree nodes, which is perhaps surprising as high degree nodes have more connections/patterns in their neighborhood that an algorithm could potentially exploit. However, as noted at the outset, there

[4]This is similar to the IDF heuristic used in information retrieval.
[5]The edges not incident to a in the cycles should be in $G_{S,train}$.

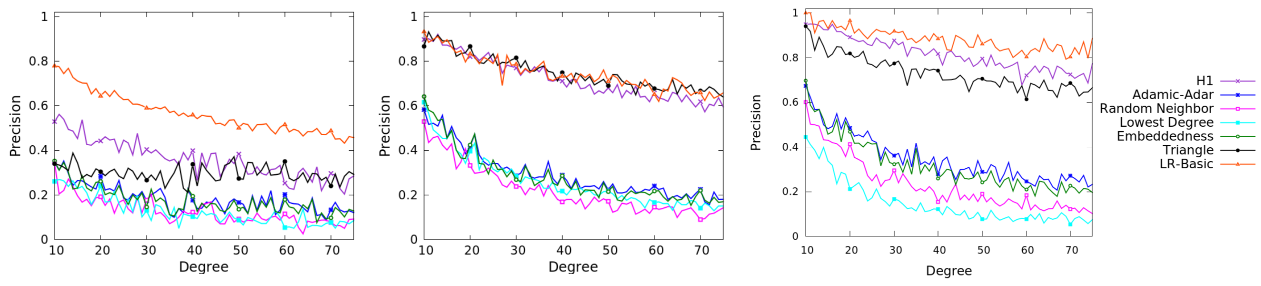

(a) Direct Message **(b) Phonebook** **(c) Email Address Book**

Figure 2: Precision at 1 for group 1 scoring functions

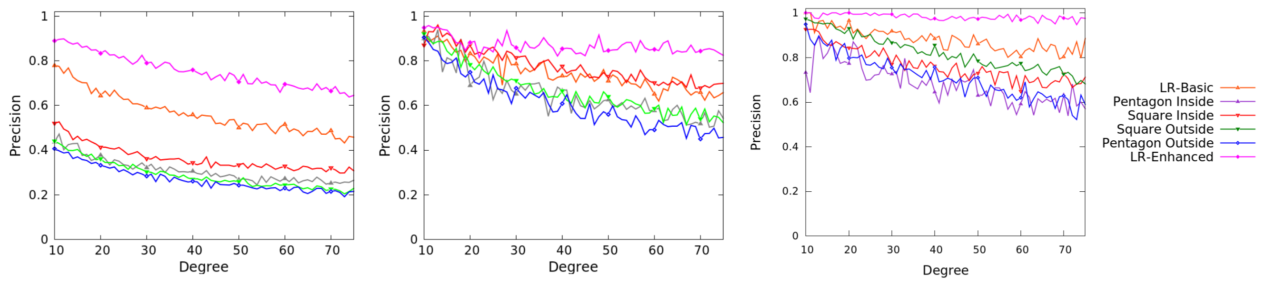

(a) Direct Message **(b) Phonebook** **(c) Email Address Book**

Figure 3: Precision at 1 for group 2 scoring functions and the linear model from group 1

is also the added difficulty from having to choose from among a larger set of neighbors, which is illustrated by the random baseline. And the latter effect is clearly stronger, as the plots indicate.

3.5 Predicting Multiple Edges

The prediction task formulated above focuses on producing a single prediction. But one might suspect that if a scoring algorithm performs well on this task, then it should also provide high precision in the setting where multiple predictions are generated. In this section, we test this hypothesis experimentally. The task we set up for the algorithm is as follows: we take a set of nodes from our test set that have at least five edges in G_S and given an algorithm's scores, we report the five neighbors with the highest score to be its prediction; thus measuring $p@5$.[6] The results of this experiment when we set G_S to be the phone book graph are shown in Figure 4.

We briefly note that the results are quite consistent with the ones for the prediction task: the Enhanced LR model outperforms the rest of the algorithms and baselines. Hence, it seems reasonable to conclude that relative performance on predicting even one edge is a good indicator of performance on predicting multiple edges.

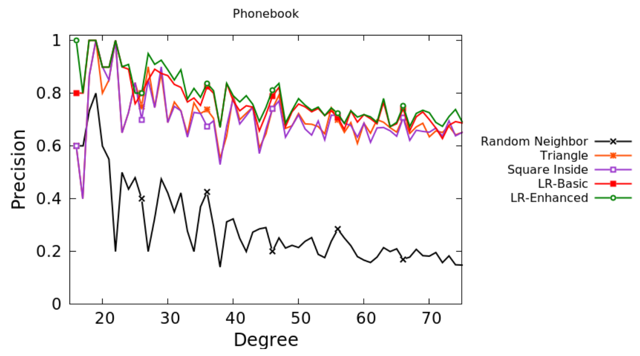

Figure 4: Precision at 5 on the phone book graph for a selection of methods. There is no node such that $d_L < 16$ and $d_S \geq 10$, therefore the plot does not start from 10. The symbols (g1) and (g2) at the end of the legends show the group of the scoring function based on table 1.

4 Theoretical Modeling

A key observation from our experimental results is that larger motifs than triangles — in particular, squares — provide a substantial performance boost on the strong tie prediction task. In this section, we aim to provide theoretical insight into why this should be the case. Specifically, in what settings can one expect richer motifs such as squares to be more useful as features for strong tie prediction?

In order to study this question analytically, we define two simple graph models that are motivated by stochastic block models. While the graphs produced by these models are much simpler than what we encounter in practice, they serve as tractable structures that capture some of the essential features of the networks in our applications. Given a graph model, we can study the usefulness of motifs by posing it as a feature sparsity question: are squares a more discriminative feature than triangles because of their higher

[6]Note that our ground truth data has only binary labels, and hence a ranking metric such as NDCG isn't applicable here.

prevalence? As we will see, this indeed turns out to be true, and we will show via analytical results and simulations that for certain parameter ranges in these graph models, squares are more discriminative features than triangles.

To start with, we define a prediction task that reflects our experimental evaluation (though it is not exactly equivalent). Given a graph $G(V, E)$ with hidden labels $L = f(e) \rightarrow \{0, 1\}$ for all $e \in E$, an algorithm is required to predict the hidden labels for edges. We will attempt to represent patterns for edges marked with label 1 via a graph generation model. The edges labeled as 1 in these models will act as strong ties and edges labeled as 0 will be the weak ties.

This task is quite similar to our empirical task, with a few differences. First, recall that in the empirical task, we had to guess only one edge as being a strong tie. Here, however, we ask for an algorithm that labels all the edges adjacent to the test node. Another difference between this model and our prediction task is the fact that in the theoretical analysis our algorithm does not have access to the labeled strong ties and will treat all the ties as weak ties. We emphasize that the main purpose of this section is to study the relative discriminative power of squares and triangles features.

4.1 Graph Models

A key step in formulating a theoretical model is to have a graph model that abstracts some of the important structural properties of friendship structures in real-world networks. Our approach is to use "planted community" models so that there is a clear structure that an algorithm can learn. Furthermore, in addition to the planted structure, we also need to appropriately represent the sparsity and noisiness of data represented in online ties of the real-world offline networks. Hence, in all the models proposed here, the underlying friendship structure in the graph is perturbed via sparsification and by adding noisy edges to the graph.

4.1.1 Single Planted Model

We start with a basic model, which we term the *single planted model*. This is a stochastic block model graph with n nodes and $\lceil \frac{n}{c} \rceil$ communities each consisting of c nodes. For parameters p, q, and r, the probability of an edge between nodes in the same community is $p\frac{q}{\sqrt{c}}$, and the probability of an edge between nodes in different communities is r.

The graph generated by this model constitutes G_L, and the subgraph consisting only of edges inside communities is G_S. We can then imagine removing edges incident to a subset of nodes V_{test} in G_S, corresponding to the isolated nodes in our prediction task.

We can think of the edge probabiltiy $p\frac{q}{\sqrt{c}}$ inside communities arising as follows: we imagine p as the probability that each pair of nodes within a community knows each other, and $\frac{q}{\sqrt{c}}$ as the probability that two such people in fact form a link between each other on the platform. This second filtering of the links via $\frac{q}{\sqrt{c}}$ makes the task more realistic and more challenging.

4.1.2 Double Planted Model

This model is an extension of the single planted model. We create two different random graphs G_1 and G_2 using the single planted model. We call the subsets of the edges inside the community ${G_1}_S$ and ${G_2}_S$. The union of ${G_1}_S$ and ${G_2}_S$ will create our graph G_S. Edges between two nodes that do not share a community are added with probability r. In this case each node is in exactly two communities. The final graph created by this process will be G_L. We call the communities in G_L that come from ${G_1}_S$ the Type-1 Group, and the communities that come from ${G_2}_S$ the Type-2 Group.

4.2 Theoretical Analysis

Now we theoretically analyze the performance of squares and triangles as predictors for finding edges in G_S in the planted models proposed above. Throughout this analysis, we will set the random noise edge probability as $r = \frac{\ln n}{n}$, and the group size to be $c = \alpha_1 \ln n$. From this point on we define $\rho = pq$. Due to similarity between the proofs for the Single and Double Planted Model we will state our claims without proofs for the Single Planted Model, and provide more details for the Double Planted Model.

We will show that in these models squares are on average a more discriminative feature than triangles. In particular, we will make this claim by examining the gap between the expected value of the two features for edges within a group versus edges between groups. Given an edge (x, y), denote the number of triangles and squares that the edge belongs to as $\Delta(x, y)$ and $\Box(x, y)$.

4.2.1 Single Planted Model

THEOREM 1. *For all edges (x, y), we have $E[\Delta(x, y)] < 1$. For edges that go between different communities we have $E[\Box(x, y)] < 1$, and for edges in the same community we have $E[\Box(x, y)] > \left(1 - \frac{5}{n}\right)\sqrt{c}\rho^3 \simeq \sqrt{c}\rho^3$.*

Thus, edges inside and between groups have a significant difference in the expected number of squares they are involved in, roughly equal to $\sqrt{c}\rho^3$. Hence, in the single planted model the squares feature is expected to be more discriminative than triangles.

The functions Δ and $\Box$ have an integer range, and for these features to be distinguishable they have to be non-zero, and the probability of an edge outside a group being in a triangle or square converges to zero. So the power of the triangle/square feature is equivalent to the probability of being in a triangle/square. For an an edge inside a group, the probability it is in a triangle is $1-(1-(\frac{\rho}{\sqrt{c}})^2)^{c-2}$ and the probability it is in a square is $1 - (1 - (\frac{\rho}{\sqrt{c}})^3)^{(c-2)(c-3)}$. The latter is much larger for sparser (smaller ρ) graphs leading to another indication that squares are a better feature than triangles.

4.2.2 Double Planted Model

THEOREM 2. *In the double planted model, $E[\Delta(x, y)] < 1$ and $E[\Box(x, y)] < 1$ for all edges (x, y) where x and y are not in the same community. For edges (x, y) where x and y are in the same community, $E[\Delta(x, y)] < 2$ and $E[\Box(x, y)] > \sqrt{c}\rho^3$.*

We start by stating two basic properties of the double planted model, formalized in the following lemmas. We skip the proofs as they are based upon a standard application of Chernoff bounds.

LEMMA 1. *For a sufficiently large constant $\alpha_1(> \frac{4.1}{\delta^2})$, with high probability($> 1-\frac{2}{cn}$), each group's size is in $[(1-\delta)c, (1+\delta)c]$.*

LEMMA 2. *For a sufficiently large constant $\alpha_1(> \frac{4.1}{\delta^2})$, with high probability, no Type-1 group has an intersection of size more than $\alpha_2(\leq 3)$ with any Type-2 group.*

The above two properties provide us with the tools to analyze the expected values of the triangles and squares features.

LEMMA 3. *For any nodes x and y, we have $E[\Delta(x, y)] \leq 1$, except the case when x and y share the same group in both types, in which case $E[\Delta(x, y)] \leq 2$. However, this latter event is rare.*

PROOF. These are the three cases we need to analyze:
x and y have two common groups: The probability of x and y sharing both groups is $(\frac{c}{n})^2$, and conditioned on that, we can upper-bound $E[\Delta(x, y)]$ by: $2\frac{c}{n}(\frac{\rho}{\sqrt{c}})^2 + (\frac{n-c}{n})^2(\frac{\ln n}{n})^2 < 2$.

x and y are in the same group: The third node z, can be in the same group as x and y, can share a group with only one of them or be an outsider to both nodes. The upper bound for the probability of any of these events happening is $\frac{2c}{n}$, $\frac{c}{n}$ and $\frac{n-c}{n}$. So the probability of triangle (x, y, z) existing is:

$$\frac{c}{n}(\frac{\rho}{\sqrt{c}})^2 + 2\frac{c}{n}\frac{n-c}{n}(\frac{\rho}{\sqrt{c}})(\frac{\ln n}{n}) + \frac{(n-c)}{n}\frac{n-2c}{n}(\frac{\ln n}{n})^2$$

By multiplying $(n-2)$ by the value above, we will find an upper-bound for $E[\Delta(x,y)]$ which is smaller than 1.
x and y are in different groups: Each third node z, can be in the same Type 1 group with x and the same Type 2 group with y or vice-versa, it can also share a group with either one of x or y but not both, or it can be an outsider to both nodes. An upper-bound for the probability of having triangle (x, y, z) is:

$$2(\frac{c}{n})^2(\frac{\rho}{\sqrt{c}})^2 + 2\frac{2c}{n}(\frac{n-c}{n})(\frac{\rho}{\sqrt{c}})(\frac{\ln n}{n}) + (\frac{(n-2c)}{n})^2(\frac{\ln n}{n})^2$$

Now if we multiply this by $n-2$ it will be the expected number of triangles which is less than 1. $\square$

In summary, for the common cases, $E[\Delta(x,y)] < 1$, and even for the rare case in which x and y have two groups in common, $E[\Delta(x,y)] < 2$. Thus, one might not expect triangles to be a useful feature in discriminating between the two kinds of ties.

Now, we present an analysis for the use of squares as features.

LEMMA 4. *If x and y are in a different group, $E[\square(x,y)] < 1$ and if they share a group, $E[\square(x,y)] \geq \sqrt{c}\rho^3$.*

PROOF. We will analyze this via a case analysis, as before:
x and y are in the same group: The number of squares including (x, y) in this case is lower-bounded by the expected number of squares when all four nodes are inside the same group. The probability of the other two nodes being in the same group is $(\frac{c}{n})^2$ so the probability of a square with the specific ordering of x, u, v, y will be $(\frac{c}{n})^2(\frac{\rho}{\sqrt{c}})^3 = \frac{\sqrt{c}\rho^3}{n^2}$.
There are $(n-2)(n-3)$ candidate pairs leading to the claimed lower-bound. If these two nodes share two groups then with a similar method and using Lemma 2 we can get a lower-bound of $2\sqrt{c}\rho^3$.
x and y are in different groups: When x and y are in different groups, there are two ways a square can form that includes (x, y). The first way is for the square to include an edge whose ends do not share a group. The second is for each of the four edges to have ends that share a group. Note that this second situation is not possible in the single planted model, but becomes possible in the double planted model whenever there are two other nodes u and v where (x, u),(u, v) and (v, y) each have a group in common. We will call such a pair (u, v) a *potential bad pair* for (x, y).

The case in which the square involves an edge whose ends do not share a group is the easier case; the expected number of such squares is very small due to the low probability on such cross-group edges, and we omit the details here. We now consider the case of a square whose edges lie within groups; we bound the expected number of such squares by bounding the number of potential bad pairs for two nodes.

We know that each of x and y have at most $2c(1+\delta)$ shared group members. A neighbor of x and a neighbor of y should be in the same group to create a bad pair. We name the groups that exclude x and y, $S_{j,1}, \ldots, S_{j,\frac{n}{c}-2}$ where $j \in \{1, 2\}$ denotes which group type it is, and the groups including x and y as $S_{1,x}, S_{2,x}, S_{1,y}, S_{2,y}$. We know that the number of potential bad pairs is:

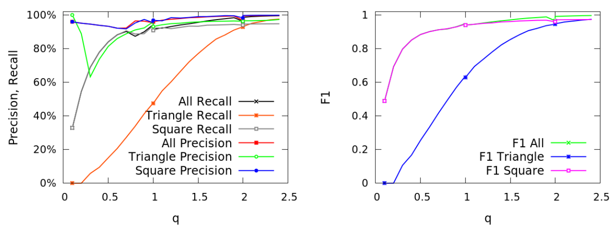

(a) Single Planted Model

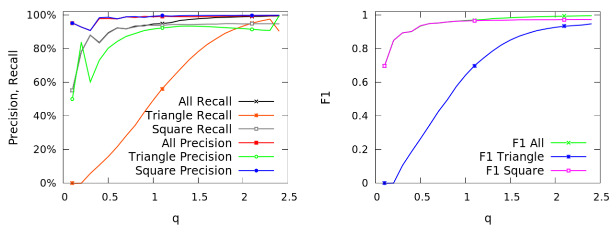

(b) Double Planted Model

Figure 7: Precision, recall and F1 score when $p = 0.85$ and variable q. (a) Single planted model (b) Double planted model

$$\sum_{j=1}^{2}[|S_{j,x} \cap S_{3-j,y}| + \sum_{i=1}^{\frac{n}{c}-2}|S_{j,x} \cap S_{(3-j),i}||S_{j,y} \cap S_{(3-j),i}|]$$

So by Lemma 2 we know, the terms $|S_{1,x} \cap S_{2,y}|$ and $|S_{2,x} \cap S_{1,y}|$ are upper bounded by a small constant. We also know $|S_{j,y} \cap S_{3-j,i}|$ and $|S_{j,x} \cap S_{3-j,i}|$ for $1 \leq j \leq 2$, are non-zero for at most $(1+\delta)c$ terms and when they are non-zero, By Lemma 2 we know that they are bounded by a small constant. Therefore, the inner sum will be at most $\mathcal{O}(c)$. Therefore, the expected number of potential bad pairs is $\mathcal{O}(c)$ which means it is less than γc (where $\gamma << 2\alpha_2^2$) with high probability.[7] Now that the grouping is done we add the edge probabilities. Since each edge is inside a group it will exist with probability $\frac{\rho}{\sqrt{c}}$ which means the expected number of bad squares is $\gamma c(\frac{\rho}{\sqrt{c}})^3 < \frac{2\alpha_2^2\rho^3}{\sqrt{c}}$. This number for a large enough n is smaller than 1. $\square$

The separation between $E[\square(x,y)]$ and $E[\Delta(x,y)]$ is as in the single planted model, and on average, we would expect the squares feature to be more discriminative compared to the triangles feature. Hence, even with these simple planted models, we observe a phenomenon where the sparsity of the triangles feature might limit its usefulness as a feature compared to squares.

4.3 Simulation Results

The theoretical results presented above show a separation in the behavior of the expected number of triangles and squares containing different kinds of edges. We now perform computational simulations to see how these separations in expectation translate into probabilistic outcomes with concrete values for the parameters.

For all these simulations, we use the prediction framework from the previous section. In particular, we use the number of triangles, number of squares, and their logarithms, both separately and combined together, as features. Then, as before, we train an LR model that is then used to make the predictions on the test set.

Given our theoretical results, we expect a parameter range where the dominant feature changes from triangles to squares. Hence,

[7]By applying the Chernoff bounds to two groups of Type-1 having intersection in a Type-2 group we can easily get a bound of $\frac{\alpha_2^2}{2}$

we run an experiment for each parameter to understand how this switch happens. In each of our experiments, we vary the chosen parameter over a wide range while keeping all the other parameters of the model fixed. We observe that for most of our parameters, the relative usefulness of the triangles and squares remains unchanged throughout the range. The only parameters that have an effect on the features' relative usefulness are the ones that affect the sparsity of the resulting graph.

The primary parameter of interest in the planted models is q, since the graph gets sparser as q gets smaller. Hence, in our presentation below we fix the rest of the parameters and only study the effect of q in the two planted models. We use the specified generative process for each model to build hundreds of train and test graphs. As suggested by Figure 7 the squares features tend to outperform the triangles when the graph is sparse. In these simulations we choose $n = 4000$, $r = \frac{\ln(n)}{n}$, the expected size for the groups c to be 30, $p = 0.85$ and values in $[0.1, 2.5]$ with a step of 0.1 for q.

5 Conclusion

In this work, we use information about a dense graph G_L composed primarily of weak ties to fill in the strong ties in a sparse graph G_S, using the frequency of small subgraphs as features. We achieve high precision on this prediction task; however, we need to go beyond structures based on triangles — as in standard approaches for strong-tie prediction — and look at subgraphs on larger numbers of nodes. The methodology seems general enough to apply to many other settings as well.

The relative usefulness of the network structures also presents a clear trade-off between noisiness and sparsity: from our results it is evident that small structures that are in direct proximity to the target node have a higher signal strength than structures that involve nodes that are farther off. At the same time, these structures tend to be sparse, and hence in some settings more abundant structures such as squares are more useful for filling in a sparsely populated graph. Our theoretical models and results demonstrate contexts where this can be shown to be the case analytically.

The setting discussed here also opens up several new questions. In particular, is it possible to quantify the properties of the relationship between G_L and G_S that are necessary for training on G_L to be useful for filling in G_S? We also note that we experimented using multiple graphs to predict edges in G_S and we only observed a small ($\sim 1\%$) increase in precision. This leads to the possibility that an understanding of the overlap properties among graphs might indicate when the use of multiple graphs could be effective for these types of prediction tasks.

6 References

[1] L. Backstrom and J. M. Kleinberg. Romantic partnerships and the dispersion of social ties: A network analysis of relationship status on facebook. In *ACM CSCW*, 2014.

[2] J. Bobadilla, F. Ortega, A. Hernando, and J. Bernal. A collaborative filtering approach to mitigate the new user cold start problem. *Knowledge-Based Systems*, 26:225–238, 2012.

[3] C. Borgs, J. T. Chayes, L. Lovasz, V. Sos, B. Szegedy, and K. Vesztergombi. Counting graph homomorphisms. In M. Klazar, J. Kratochvil, M. Loebl, J. Matousek, R. Thomas, and P. Valtr, editors, *Topics in Discrete Mathematics*. Springer, 2006.

[4] A. Condon and R. M. Karp. Algorithms for graph partitioning on the planted partition model. *Random Structures and Algorithms*, 2001.

[5] J. Dean and S. Ghemawat. Mapreduce: simplified data processing on large clusters. *Communications of the ACM*, 51(1):107–113, 2008.

[6] N. Eagle, A. S. Pentland, and D. Lazer. Inferring friendship network structure by using mobile phone data. *Proc. Natl. Acad. Sci. USA*, 106(36), 2009.

[7] K. Faust. A puzzle concerning triads in social networks: Graph constraints and the triad census. *Social Networks*, 32(3), 2010.

[8] P. Flajolet, É. Fusy, O. Gandouet, and F. Meunier. Hyperloglog: the analysis of a near-optimal cardinality estimation algorithm. *DMTCS Proceedings*, 2008.

[9] E. Gilbert. Predicting tie strength in a new medium. In *CSCW*. ACM, 2012.

[10] E. Gilbert and K. Karahalios. Predicting tie strength with social media. In *SIGCHI*. ACM, 2009.

[11] M. Granovetter. The strength of weak ties. *American Journal of Sociology*, 78, 1973.

[12] T. Joachims. Transductive learning via spectral graph partitioning. In *ICML*, 2003.

[13] J. J. Jones, J. E. Settle, R. M. Bond, C. J. Fariss, C. Marlow, and J. H. Fowler. Inferring tie strength from online directed behavior. *PLoS ONE*, Jan. 2013.

[14] M. Kim and J. Leskovec. Modeling social networks with node attributes using the multiplicative attribute graph model. In *UAI*, 2011.

[15] M. Kim and J. Leskovec. The network completion problem: Inferring missing nodes and edges in networks. In *SIAM*, 2011.

[16] M. Kuramochi and G. Karypis. Frequent subgraph discovery. In *ICDM*, 2001.

[17] L. Liu, J. Tang, J. Han, M. Jiang, and S. Yang. Mining topic-level influence in heterogeneous networks. In *CIKM*, 2010.

[18] P. V. Marsden and K. E. Campbell. Measuring tie stength. *Social Forces*, 63(2), Dec. 1984.

[19] F. McSherry. Spectral partitioning of random graphs. In *FOCS*, 2001.

[20] R. Milo, S. Shen-Orr, S. Itzkovitz, N. Kashtan, D. Chklovskii, and U. Alon. Network motifs: Simple building blocks of complex networks. *Science*, 298(5594), Oct. 2002.

[21] F. K. C. Moore, E. Mossel, J. Neeman, A. Sly, L. Zdeborová, and P. Zhang. Spectral redemption in clustering sparse networks. *Proc. Natl. Acad. Sci. USA*, 110(52), 2013.

[22] E. Mossel, J. Neeman, and A. Sly. Belief propagation, robust reconstruction, and optimal recovery of block models. *COLT*, 2014.

[23] A. I. Schein, A. Popescul, L. H. Ungar, and D. M. Pennock. Methods and metrics for cold-start recommendations. In *Proceedings of the 25th annual international ACM SIGIR conference on Research and development in information retrieval*, pages 253–260. ACM, 2002.

[24] S. Sedhain, S. Sanner, D. Braziunas, L. Xie, and J. Christensen. Social collaborative filtering for cold-start recommendations. In *Proceedings of the 8th ACM Conference on Recommender systems*, pages 345–348. ACM, 2014.

[25] C. Seshadhri, A. Pinar, and T. G. Kolda. Triadic measures on graphs: The power of wedge sampling. In *SIAM*

International Conference on Data Mining (SDM), pages 10–18. SIAM, 2013.

[26] S. Sintos and P. Tsaparas. Using strong triadic closure to characterize ties in social networks. In *SIGKDD*, 2014.

[27] Y. Sun, R. Barber, M. Gupta, C. C. Aggarwal, and J. Han. Co-author relationship prediction in heterogeneous bibliographic networks. In *International Conference on Advances in Social Networks Analysis and Mining, ASONAM 2011, Kaohsiung, Taiwan, 25-27 July 2011*, pages 121–128, 2011.

[28] J. Tang, T. Lou, and J. M. Kleinberg. Inferring social ties across heterogenous networks. In *WSDM*, 2012.

[29] J. Ugander, L. Backstrom, and J. Kleinberg. Subgraph frequencies: Mapping the empirical and extremal geography of large graph collections. In *WWW*, 2013.

[30] C. Wang, J. Han, Y. Jia, J. Tang, D. Zhang, Y. Yu, and J. Guo. Mining advisor-advisee relationships from research publication networks. In *Proceedings of the 16th ACM SIGKDD International Conference on Knowledge Discovery and Data Mining, Washington, DC, USA, July 25-28, 2010*, pages 203–212, 2010.

[31] X. Yan and J. Han. gspan: Graph-based substructure pattern mining. In *ICDM*, 2002.

[32] X. Zhu and Z. Ghahramani. Learning from labeled and unlabeled data with label propagation. Technical report, Carnegie Mellon University, 2002.

7 Appendix

7.1 Computing Squares on Large Graphs

Computing the exact number of squares on large graphs can be a challenging problem. This connects to a large literature on counting triangles and other network motifs, but the size of the graph in our problem poses challenges for even the most efficient known techniques. Here, we briefly point out a scalable heuristic that can compute the feature using a randomized algorithm by utilizing HyperLogLog sketches [8]. This approach does not provide good worst case guarantees as it is, but in practice we've observed reasonable performance from the heuristic. We also note that the counts produced by these sketches are fed to a classifier, which provides an additional layer of robustness for error.

Consider a node a with direct neighbors B in G_L, and second degree neighbors C (excluding the nodes distance two away that are in B). We need to compute the squares feature for each $b \in B$. A naive method of computing this would involve forming a list of b's neighbors that are also in C, and doing pairwise intersections between the lists of all b's. We note that one can flip this computation around, with each $c \in C$ having a list of neighbors that is intersected with the set B, as then each pair in the resulting list has a unique square path.
This idea can be implemented efficiently with HyperLogLog sketches that implement intersections [8]. In particular, each c computes a sketch of its neighbors, and each b is annotated with a sketch of B's. Then, for an existing (b, c) edge, the intersection of these sketches is exactly one more than the number of squares that b participates in. This computation can be implemented efficiently in MapReduce [5].

We re-emphasize that in our experiments in this work, we do not use this approximation (since the sample size was tractable with exact computation). We note this algorithm here to demonstrate that the squares feature can be computed on extremely large graphs in an efficient manner.